Behavior of the relativistic angular and energy distributions of atoms exposed to a strong and low-frequency circularly polarized laser field

Tatjana B. Miladinović and Violeta M. Petrović*

Department of Physics, Faculty of Science, Kragujevac University, Radoja Domanovića 12, 34000 Kragujevac, Serbia

**Corresponding author: violeta.petrovickg@gmail.com*

Received February 27, 2015; accepted May 27, 2015; posted online June 15, 2015

In this Letter, we focus on the theoretical analysis of the relativistic energy and angular distributions of the ejected photoelectrons during the relativistic tunnel ionization of atoms by intense, circularly polarized light. We make a small modification of the general analytical expressions for these distributions. The role of the initial momentum, the ponderomotive potential, and the Stark shift are considered. We also present the maximal angle of electron emission.

OCIS codes: 020.2649, 020.4180.
doi: 10.3788/COL201513.070005.

During the last decade, many papers have provided a detailed picture of the process of tunneling[1–3] ionization of atoms, atomic ions, and molecules. Also, the photoelectron momentum distribution produced in a circularly polarized laser field has been imposed as a new issue, both theoretically and experimentally. Smeenk *et al.*[4] measured the photoelectron momentum and momentum transfer from the photon field to the electron–ion system, while Chelkowski *et al.*[5] investigated photon-momentum sharing between an electron and an ion following different photoionization regimes. Both papers suggest there is unexplored physics to be studied.

Today, strong lasers provide intensities on the order of 10^{22} W cm^{-2}[6–9]. In such fields an electron acquires a velocity comparable to the speed of light and, taking relativistic effects into account, becomes fundamentally important. The field with such intensity can exceed the atomic field $F_a = 5.14 \times 10^9$ V/cm by several orders of magnitude and are capable of creating multivalent ions with charges $Z = 40$–60, for which the binding energy of the ground level is also comparable with the electron rest energy. However, for $Z \geq 10$ relativistic effects must be taken into account[10].

The ionization of atoms and atomic ions by intense laser fields was brought to researchers' attention a long time ago[11–13]. The theory of these processes was started by Keldysh[14], where the tunnel effect in an alternating electric field and the multiphoton ionization of atoms were found to be the limiting cases of the nonlinear photoionization process. The range $\gamma = (I_p/2U_p)^{1/2} \ll 1$ corresponds to the tunneling ionization limit, while the multiphoton regime in which the electron climbs a ladder of electronic states to reach the continuum through multiphoton absorption corresponding to $\gamma \gg 1$[14]. Here, U_p is ponderomotive potential and I_p is the ionization potential of the considered atom, or of the atomic ion. However, the laser irradiation influences the ionization potential of an atom. Increasing field intensity also increases the ionization potential. We considered this influence through the ponderomotive potential and the Stark shift in the relativistic domain. The ponderomotive potential presents the time-averaged kinetic energy of the electron, $U_p^{\mathrm{nonrel}} = \frac{F^2}{2\omega^2}$, where F and ω are the strength and the frequency, respectively, of the electromagnetic field. In the relativistic domain ponderomotive potential may be written in the form $U_p^{\mathrm{rel}} = \sqrt{\mathrm{c}^4 + 2\mathrm{c}^2 U_p^{\mathrm{nonrel}}} - \mathrm{c}^2$[15], where c is the speed of light. The Stark effect has the same form as in the nonrelativistic domain, $E_{\mathrm{St}} = \alpha F^2/4$[16], where E_{St} is the shift caused by the linear Stark effect and α is the static polarizability of the atom[17]. To account for these two effects, we replaced unperturbed relativistic ionization potential $I_p^{\mathrm{rel}} = \mathrm{c}^2 - \sqrt{\mathrm{c}^4 - Z^2\mathrm{c}^2}$[18] with the shifted, corrected relativistic effective ionization potential and obtained

$$I_p^{\mathrm{rel,eff}} = \mathrm{c}^2 - \sqrt{\mathrm{c}^4 - Z^2\mathrm{c}^2} + \left(\sqrt{\mathrm{c}^4 + 2\mathrm{c}^2 U_p^{\mathrm{nonrel}}} - \mathrm{c}^2\right) + \alpha F^2/4. \quad (1)$$

In this Letter we discuss the influence of the effective ionization potential on the relativistic angular and energy distribution of the ejected photoelectrons. We restrict ourselves to the case of the ejection of an electron along the polarization axis only, since most of electrons are ejected in this direction. We will be interested in the ejection of a small number of electrons where relativistic effects are important. In the atomic system of units, the electron mass, m_e, charge e and $\hbar$ are equal to 1 and $\mathrm{c} = 137.02$ is the speed of light.

The angular distribution is found to be[19]

$$W^{\mathrm{rel}}(\theta) = W^{\mathrm{nonrel}} \exp\left[-\left(1+\left(\frac{\mathcal{E}F}{2\omega \mathrm{c}}\right)^2\right)\frac{\mathcal{E}F\sqrt{2I_p}}{\omega^2}(\theta-\theta_{\max})^2\right], \quad (2)$$

where $0 < \varepsilon < 1$ is the ellipticity of the laser radiation. A circularly polarized laser beam is a coherent superposition of photons with definite helicity, e.g., $\varepsilon = 1$. Term θ is the scattering angle of the ejected photoelectrons and $\theta_{\max}$ is angle on which the maximum of the angular distribution in the relativistic case is found

$$\theta_{\max} = \arctan\frac{\mathcal{E}F}{2\omega \mathrm{c}}. \quad (3)$$

Term W^{nonrel} is the nonrelativistic tunneling transition rate for the circularly polarized laser field which can be calculated, for example, in the framework of Ammosov–Delone–Krainov (ADK) theory in the well-known form[20] $W = \frac{FD^2}{8\pi Z}\exp[-\frac{2Z^3}{3n_{ef}^3 F}]$, where $D \equiv (4eZ^3/Fn_{ef}^4)^{n_{ef}}$; n_{ef} is the effective quantum number, $n_{ef} = Z/(2I_p)$; Z is the ion charge. With included nonzero initial momentum of the ejected photoelectrons the aforementioned transition rate becomes[21]

$$W^{\mathrm{nonrel}} = \frac{FD^2}{8\pi Z}\exp\left[-\frac{2Z^3}{3n_{ef}^3 F}-\frac{p^2\gamma^3}{3\omega}\right], \quad (4)$$

where p is the initial momentum of the ejected photoelectrons. For purposes of calculations it is convenient to use the parabolic coordinate[22]. This is useful in investigating a number of problems as well as angular and energy distributions of photoelectrons in an external electric field. If a system's total energy is independent of the coordinate η then momentum is conserved along the classical path, i.e., $p_\eta = p$[22], where $p = \frac{1}{2}(\sqrt{F\eta-1} - \frac{1}{\eta\sqrt{F\eta-1}})$ and η is the parabolic coordinate, $\eta > 1/F$[23].

Energy spectra of relativistic electrons in the tunneling ionization of multicharged atomic ions had been found in Ref. [24] for circularly polarized light and in Ref. [25].

The relativistic energy distribution at this angle is determined as[19]

$$W^{\mathrm{rel}}(E) = W^{\mathrm{nonrel}} \exp\left[-\frac{\gamma}{2\omega U_p^{\mathrm{rel}}}(E-U_p^{\mathrm{rel}})^2\right], \quad (5)$$

where E is the kinetic energies of the ejected electrons, and in the case when this energy is less than the rest energy of the electrons is determined as[25]

$$E = \sqrt{p^2\mathrm{c}^2+\mathrm{c}^4} - \mathrm{c}^2. \quad (6)$$

The relativistic energy distribution [Eq. (5)] along the field strength decreases exponentially in accordance with the electron kinetic energy.

We discussed the influence of the relativistic ponderomotive and the Stark shift effects on the angular and the energy distributions of the ejected photoelectrons in the field of laser radiation. The case of low-frequency circularly polarized laser field is considered. Wavelength of 800 nm produced by a titanium:sapphire-based laser system is considered and according to Reiss, for a laser with this wavelength relativistic effects appears up to $I = 10^{17}$ W cm^{-2}[26,27]. For our calculation the value of Z was fixed at 10. The analysis was performed for the atom argon, Ar. Figures 1–6 should be considered only as an illustration of the enhancement effects.

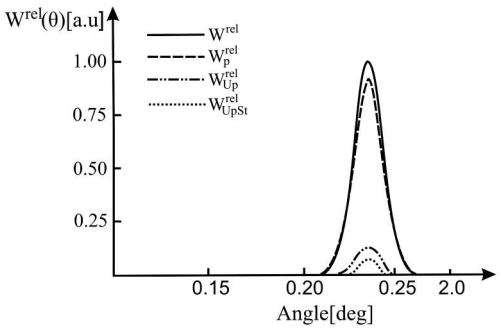

Fig. 1. Angular distribution $W^{\mathrm{rel}}(\theta)$ for fixed $I = 10^{18}$ W cm^{-2} and $\eta = 0.35$ versus the scattering angle θ.

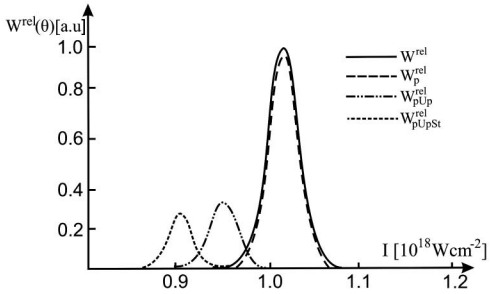

Fig. 2. Relativistic angular distribution $W^{\mathrm{rel}}(\theta)$ for the fixed scattering angle $\theta = 0.22$ and the parabolic coordinate $\eta = 0.35$ versus the laser field intensity I.

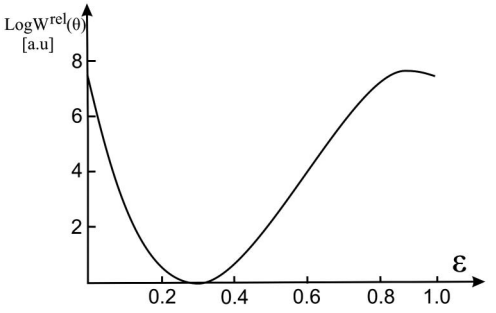

Fig. 3. Relativistic angular distribution Log $W^{\mathrm{rel}}(\theta)$ versus the ellipticity, ε, for the fixed scattering angle $\theta = 0.22$, the parabolic coordinate $\eta = 0.35$, and the laser field intensity $I = 10^{18}$ W cm^{-2}.

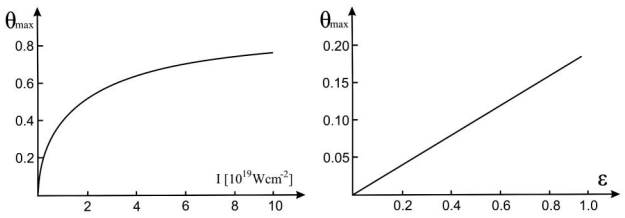

Fig. 4. (a) Maximal scattering angle $\theta_{\max}$ versus laser field intensity I; (b) maximal scattering angle $\theta_{\max}$ versus the ellipticity, $\mathcal{E}$, for the fixed laser field intensity $I = 10^{18}$ W cm^{-2}.

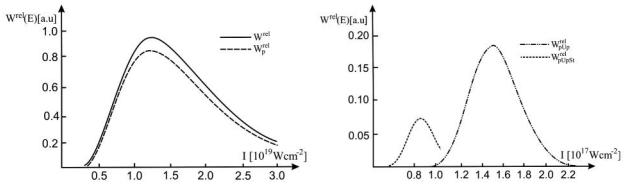

Fig. 5. Relativistic energy distribution $W^{\mathrm{rel}}(E)$ for the fixed parabolic coordinate $\eta = 10$.

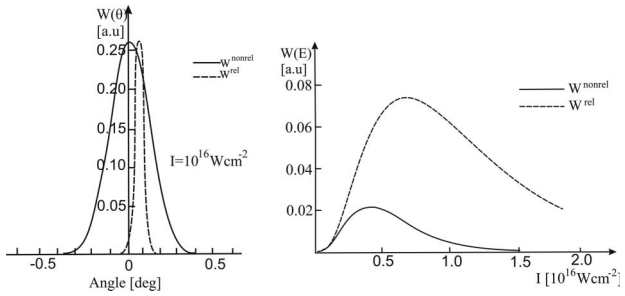

Fig. 6. Comparative review; nonrelativistic versus relativistic results of the angular $[W^{\mathrm{rel}}(\theta)$ vs $W^{\mathrm{nonrel}}(\theta)]$ and the energy distribution spectra $[W^{\mathrm{rel}}(E)$ vs $W^{\mathrm{nonrel}}(E)]$, with all included corrections for the fixed parabolic coordinates $\eta = 50$ and 100, respectively.

We started from the relativistic angular distribution of photoelectrons emitted along the laser polarization axes.

Based on Eq. (2), for a fixed laser field intensity I and the parabolic coordinate η, Fig. 1 is obtained. First we included only nonzero initial momentum of ejected electron, W_p^{rel}, then momentum and ponderomotive potential $W_{p\mathrm{Up}}^{\mathrm{rel}}$ and finally momentum, ponderomotive potential and Stark shift, $W_{p\mathrm{UpSt}}^{\mathrm{rel}}$. As can be seen the relativistic angular distribution dependence at such high field intensity occurs over a small range of scattering angles and reaches the maximal value at $\theta_{\max} = 2$. Inclusion of the aforementioned effects leads to the significant decrease in the maximal value. The relativistic angular distribution is symmetric with respect to the middle of the curve at the maximal scattering angle.

In Fig. 2 the relativistic photoelectron angular distribution, plotted in accordance with Eq. (2), for the fixed scattering angle, θ, is shown.

Here we focus on the field intensity region where all relativistic angular distributions occur. From Fig. 2, as well as from Fig. 1, we can conclude that the relativistic angular distribution of photoelectrons in the case of a circularly polarized field is very sensitive to considered effects.

We also show $W^{\mathrm{rel}}(\theta)$ as a function of the ellipticity, $\mathcal{E}$.

It is obvious that the angular distribution is strongly asymmetric along the propagation axes, (Fig. 3). This asymmetry grows with the increasing of the ellipticity.

In Fig. 4, for the sake of illustration of the angular distribution we show behavior of the maximal scattering angle [Eq. (3)].

The maximal angle $\theta_{\max}$ increases in accordance with the field intensity and reaches a plateau. With increasing of ellipticity, $\mathcal{E}$, $\theta_{\max}$ also increases. This dependence is linear. Of course, this result is specific for a considered case.

The strict relationship between the field intensity and the energy distribution is an important tool and it is described next. The theoretical dependence is obtained through Eq. (5) and corresponding graphs are shown in Fig. 5.

Let us to discuss some of the general properties of the obtained theoretical curves in Fig. 5. In presented curves all effects are included. To summarize, we can say that the effects narrow the relativistic energy distribution. As it can be seen, with increasing laser field intensity, the energy distribution approaches zero. It is seen that these energy spectra differ strongly from the spectrum without any correction, $W^{\mathrm{rel}}(E)$, and spectrum with included initial momentum only, $W_p^{\mathrm{rel}}(E)$. If the ponderomotive potential $W_{p\mathrm{Up}}^{\mathrm{rel}}(E)$ and the Stark shift of the energy of the ground state of an atom are taken into account, the curves are shifted to lower field intensities.

Finally, it is interesting to compare the results of the relativistic and nonrelativistic angular distribution spectra[20], $W^{\mathrm{rel}}(\theta)$ vsersus $W^{\mathrm{nonrel}}(\theta)$, as well as the energy distribution spectra $W^{\mathrm{rel}}(E)$ versus $W^{\mathrm{nonrel}}(E)$[28] (Fig. 6).

The laser field intensity is chosen to be near a value where the nonrelativistic and the relativistic effects can be expected.

For fixed field intensity, $I = 10^{16}$ W cm^{-2}, $W^{\mathrm{rel}}(\theta)$ has a slightly higher value than $W^{\mathrm{nonrel}}(\theta)$. In this case the maximum of $W^{\mathrm{rel}}(\theta)$ is moved to the right.

A different picture is obtained for the energy distribution spectra, $W^{\mathrm{rel}}(E)$ versus $W^{\mathrm{nonrel}}(E)$. The graph (Fig. 6) demonstrates that, for these conditions, the curves take into account both possible ionization mechanisms and as a result, the curve's maximum is shifted towards higher or lower laser field intensity.

In conclusion, the relativistic angular and energy distributions of the ejected photoelectrons are discussed in the framework of the ADK theory. For unchanged parameters, inclusion of the considered effects changes the shape of the aforementioned distributions. We show that the effects of the included corrections are significant. We also present behavior of the maximal scattering angle as a function of the field intensity. It must emphasized that the explanation of these distributions in the tunneling

ionization regime in this Letter is not restricted to the case of the argon atom. All the results can be applied to other noble atoms.

This work was supported by the Serbian Ministry of Education, Science, and Technological Development for financial support through Projects 171020 and 171021.

References

1. M. Li, L. Qin, C. Wu, L. Y. Peng, Q. Gong, and Y. Liu, Phys. Rev. A **89**, 013422 (2014).
2. A. Staudte, S. Patchkovskii, D. Pavičić, H. Akagi, O. Smirnova, D. Zeidler, M. Meckel, D. M. Villeneuve, R. Dörner, M. Yu. Ivanov, and P. B. Corkum, Phys. Rev. Lett. **102**, 033004 (2009).
3. H. W. Loon, "Photoionization of atom by intense laser fields," Ph.D. dissertation (Department of Physics, Faculty of Science, University of Malaya, Kuala Lumpur, 2014).
4. C. T. L. Smeenk, L. Arissian, B. Zhou, A. Mysyrowicz, D. M. Villeneuve, A. Staudte, and P. B. Corkum, Phys. Rev. Lett. **106**, 193002 (2011).
5. S. Chelkowski, A. D. Bandrauk, and P. B. Corkum, Phys. Rev. Lett. **113**, 263005 (2014).
6. S. W. Bahk, P. Rousseua, T. A. Planchon, V. Chvykov, G. Kalintchenko, A. Maksimchuk, G. A. Mourou, and V. Yanovsky, Opt. Lett. **29**, 2837 (2004).
7. S. W. Bahk, P. Rousseau, T. A. Planchon, V. Chvykov, G. Kalintchenko, A. Maksimchuk, G. A. Mourou, and V. Yanovsky, Appl. Phys. B **80**, 823 (2005).
8. V. Yanovsky, V. Chvykov, G. Kalinchenko, P. Rousseau, T. Planchon, T. Matsuoka, A. Maksimchuk, J. Nees, G. Cheriaux, G. Mourou, and K. Krushelnick, Opt. Express **16**, 2109 (2008).
9. V. Bagnoud, B. Aurand, A. Blazevic, S. Borneis, C. Bruske, B. Ecker, U. Eisenbarth, J. Fils, A. Frank, E. Gaul, S. Goette, C. Haefner, T. Hahn, K. Harres, H.-M. Heuck, D. Hochhaus, D. H. Hoffmann, D. Javorková, H.-J. Kluge, T. Kuehl, S. Kunzer, M. Kreutz, T. Merz-Mantwill, P. Neumayer, E. Onkels, D. Reemts, O. Rosmej, M. Roth, T. Stoehlker, A. Tauschwitz, B. Zielbauer, D. Zimmer, and K. Witte, Appl. Phys. B **100**, 137 (2010).
10. N. Milosevic, V. P. Krainov, and T. Brabec, Phys. Rev. Lett. **89**, 193001 (2002).
11. A. M. Perelomov, V. S. Popov, and M. V. Terentev, Soviet Phys. JETP **23**, 924 (1966).
12. L. Bai, T. Cui, Y. Liu, Y. Wang, D. Deng, and J. Tao, Chin. Opt. Lett. **9**, 010203 (2011).
13. H. R. Reiss, Phys. Rev. Lett. **101**, 43002 (2008).
14. L. V. Keldysh, Sov. Phys. JETP **20**, 1307 (1965).
15. I. Ghebregziabher, *Radiation and Photoelectron Dynamics in Ultrastrong Laser Fields* (Pro Quest LLC, 2008).
16. N. B. Delone and V. P. Krainov, *Multiphoton Processes in Atoms*, 2nd ed. (Springer, 2000).
17. http://ctcp.massey.ac.nz/Tablepol-2.11.pdf.
18. E. Yakaboylu, M. Klaiber, H. Bauke, K. Z. Hatsagortsyan, and H. K. Christoph, Phys. Rev. A **88**, 063421 (2013).
19. B. Piraux and K. Rzazewski, *Super Intense Laser Atom Physics* (Springer, 2008).
20. N. B. Delone and V. P. Krainov, Phys. Uspekhi **41**, 469 (1998).
21. V. M. Ristić, T. B. Miladinović, and M. M. Radulović, Laser Phys. **18**, 1183 (2008).
22. L. D. Landau and E. M. Lifshitz, *Quantum Mechanics: Non-Relativistic Theory*, 3rd ed. (Pergamon, 1991).
23. D. Bauer, *Theory of Intense Laser-Matter Interaction*, Lecture notes (Max–Planck Institute, 2006).
24. V. P. Krainov, J. Phys. B **32**, 1607 (1999).
25. V. P. Krainov, Opt. Express **2**, 268 (1998).
26. H. R. Reiss, Phys. Rev. A **63**, 013409 (2000).
27. H. R. Reiss, Opt. Express **8**, 99 (2001).
28. N. B. Delone, I. Kiyan, and V. P. Krainov, Laser Phys. **3**, 312 (1993).